


Investigation of the Viability of Different Cancer Cells on Decellularized Adipose Tissue

Esin Akbay Çetin^{1*} 

¹Department of Biology, Faculty of Science, Hacettepe University, 06800, Ankara, Türkiye

*akbayesin@gmail.com

*Orcid No: 0000-0002-0797-8322

Received: 30 November 2022

Accepted: 15 June 2023

DOI: 10.18466/cbayarfbe.1212604

Abstract

Cancer is one of the most severe diseases diagnosed in millions of people worldwide each year. Despite many studies, there is insufficient information on how tumor formation prevents cancer treatment development. Although clinical trials are the most effective way to examine tumor formation and test anti-tumor drugs, ethical and safety limitations prevent this method from being widely used. This study aims to test the cellular behavior of different cancer cell lines on the platform obtained from decellularized adipose tissue *in vitro*. Detergent-based decellularization protocol applied to adipose tissue and cancer cell lines were seeded on obtained extracellular matrixes. Cell viability and apoptosis were observed by 3-(4,5-dimethylthiazol-2-yl)-2,5-diphenyltetrazolium bromide (MTT) assay and Acridine orange/Propidium iodide double staining, respectively. Also, cell-cell and cell-matrix interactions were investigated via pan-cadherin immunostaining. All cancer cell lines were also seeded in a cell culture dish to compare three-dimensional culture results with two-dimensional culture. As a result, the decellularization protocol allowed the original structure of the tissue scaffold to be preserved. According to cell viability analysis and immunocytochemical staining results, glioblastoma cell line (T98G) and human hepatoma cell line (Hep3B) were observed to have higher adhesion and viability potential than colon adenocarcinoma cell line (WiDr) on the tissue matrix obtained. With this study, it can be said that different cancer cells have different behaviors on decellularized matrixes. Finally, developing *in vitro* models as a more economical, scalable, and reproducible way to test drugs and therapeutics is crucial for successful clinical translation.

Keywords: Adipose tissue, Cancer cell lines, Decellularization, Extracellular matrix, Three-dimensional culture model

1. Introduction

In recent years, it has been known that cancer is one of the leading causes of death, especially in developed countries. Significant efforts have been made to overcome this disease, which has not yet had a definitive cure [1]. These efforts focused mainly on unlimited replication, causes of cell migration, genetic mutations, and intracellular signaling [2]. Cancer has recently begun to be considered a tissue to understand its general mechanism better. For this reason, the focus was on the extracellular matrix (ECM), critical in regulating cell behavior in cancer tissues and all tissues [3, 4].

Scientists rely on various scientific tools to test promising therapeutics and understand the biology underlying health and disease. One of the most widely used models is *in vivo* animal models.

While extensive animal experiments were the best approach until recently, different models have been preferred for ethical and scientific reasons [4]. Today, many three-dimensional *in vitro* cancer models are trying to be developed as a more straightforward alternative to animal models. Ideal for the three-dimensional model is to expect the three-dimensional structure of the tumor, especially the presence of cell-cell and cell-matrix interactions [5].

Recent studies in the extraction and purification of decellularized ECM from healthy tissues show that ECMs can be used for physio mimetic 3D *in vitro* tumor models in terms of their basic biomolecular properties and dynamic cancer cell-ECM interactions [6]. ECM is an important structure consisting of various protein and carbohydrate types, providing tissue-specific cellular functions and specific features for each tissue and organ type.

Functional ECMs are preferred in tissue engineering because they are a platform that will support cells and have a structure that will support the adhesion, migration, proliferation, and differentiation of cells to this platform. The difficulty of synthetic scaffolds in mimicking *in vivo* ECM structures has led to the widespread use of naturally derived ECMs. While natural ECMs are used in tissue engineering applications, they must first be cleansed from all cells (by decellularization) [7]. It has been also reported that the composition and architecture of the ECM may vary according to the tumor type and stage of progression [6, 8]. The resulting ECMs have a dynamic structure. It is important to note that ECMs serve many functions, including scaffolding, storing growth factors that are pro- and anti-tumor, and regulating differentiation, immune stimulation, and tumor migration [9-11].

Decellularization methods include physical, chemical, enzymatic, or combined use. Which method will be used is chosen by the characteristics of the target tissue/organ. All these methods have advantages and limitations, but the common use is to cleanse the tissue from all its cells entirely and to have the least component loss and damage to the ECM during this process [5]. The standardized adipose tissue decellularization method we reported was preferred in this study as it is reliable [12].

This study obtained natural scaffolds by decellularizing rat adipose tissue to mimic the *in vivo* microenvironment. It is aimed to study and compare the proliferation and adhesion profiles of different cancer cells (T98G, WiDr, and Hep3B) on this natural scaffold.

2. Materials and Methods

2.1. Obtaining Adipose Tissue

Within the scope of the study, 5 *Wistar albino* rats (300-350 gr) were used with the approval of the Hacettepe University Animal Care and Use Committee (Permit no. 2012/52). The rats were humanely killed after intraperitoneal injection with an overdose of anesthesia (10% ketamine - 2% xylazine). Subcutaneous adipose tissues isolated under sterile conditions were washed twice with sterile phosphate buffer solution (PBS) before being cut into 5 cm x 5 cm pieces. Upon the collection of adipose tissue pieces, PBS containing 1% penicillin-streptomycin (P/S) was used as a solution to preserve the tissues until the pieces were decellularized at +4 °C.

2.2. Decellularization Method

Rat subcutaneous adipose tissues, which were decellularized using the standardized decellularization method in our previous studies, were cut into pieces after they were obtained and stored under appropriate conditions until the experiments were started [12-14].

Briefly, samples were treated in 0.5% sodium dodecyl sulfate (SDS) solution for two days.

Following this application, it was exposed to 1% SDS solution for 24 hours, and in the last step, 1% TritonX-100 solution was used for one hour. Between each step, samples were washed with PBS. The decellularized samples were washed twice with PBS and stored in PBS containing 1% P/S at +4 °C until lyophilization. Non-decellularized adipose tissue samples were used as a control group.

2.3. Histological Staining

Histological analyzes were performed to observe the effectiveness of decellularization. Hematoxylin, Eosin (H&E), and Masson Trichrome (MT) staining methods were used. Briefly, 10% formalin was used for fixation. Both decellularized control and decellularized tissue matrices were fixed. The fixed samples were passed through the alcohol batch, embedded in paraffin blocks, and cut into 5 µm slices with a microtome. Sections were stained with both stains according to the protocols and observed under a light microscope (Leica DM100, Germany).

2.4. Lyophilization and Sterilization Methods

Before lyophilization, all samples obtained were stored at -80 °C overnight. For the lyophilization process, the samples were dried in a freeze dryer (Chris Alpha1-2 LD plus, M Christ GmbH, Germany) for 24 h. The lyophilized samples were stored at -20 °C until the stage in which the cells were seeded.

For sterilization, the lyophilized decellularized matrix was transferred to 24-well plates. All matrix surfaces were exposed to ultraviolet (UV) irradiation for 45 minutes. At the same time, parafilm, used to prevent the cells from adhering to the surface of the wells, was soaked in 70% ethanol before they were placed in the wells. Plates, the surfaces of which were coated with parafilm, were sterilized with 70% ethanol and finally exposed to UV irradiation for 20 minutes [15].

2.5. Culture of Cancer Cell Lines

The cancer cell lines that are tried to be modeled *in vitro* within the scope of this study are human brain cancer (T98G, CRL-1690™), human hepatoma (Hep3B, HB-8064™), and human colon carcinoma cell lines (WiDr, CCL-218™). All cell lines were purchased from the American Type Culture Collection (ATCC), Rockville, MD, USA. T98G and Hep3B cell lines were cultured in 75 cm² culture flasks (Corning, USA) using Dulbecco's modified Eagle's medium (DMEM) supplemented with 10% fetal bovine serum (FBS), 1% glutamine, 1% P/S while WiDr cell line was routinely cultured in high glucose DMEM supplemented with 10% FBS and 1% P/S. All cells were incubated at standard conditions of 37 °C, 95% relative humidity, and 5% CO₂.

2.6. Cell Seeding

To grow cells as two-dimensional, cells were cultured with their specific medium for each cancer cell type on culture flasks in a traditional incubator (5% CO₂, 95% humidity, 37 °C) [15]. For three-dimensional cell culture, it was determined as 2x10⁵ cells / 5 mm matrix for cell cultivation considering the literature [16, 17]. All cancer cells were trypsinized before cell seeding. Cells in a suspended state were prepared for cultivation with their specific medium. The matrices were placed in 24-well plates covered with parafilm, one for each well. A 20 µl of cell suspension was seeded onto each matrix and incubated in an incubator (37 °C / 5% CO₂) for 2 h. Finally, a 200 µl medium was added to each scaffold to maintain the density of 2x10⁵ cells/matrix inoculation [18, 19]. The matrices were stored in an incubator for 12 h before reaching the final volume of 500 µl in each well. Simultaneously decellularized control scaffolds were incubated in cell-free DMEM/F12. For equal cell seeding into each matrix, the cell suspension was gently pipetted before each use.

Acridine Orange and Propidium Iodide (AO/PI) double staining, immunocytochemical staining and MTT tests were performed at 24., 48., and 72. h following the cell cultivation. Separate matrices were used for all experiments with 3 replications.

2.7. AO/PI Staining

AO and PI double staining method was preferred to determine the apoptotic potential of cells on matrices. Briefly, the culture medium on the matrix was removed at 24, 48, and 72 h. Then, the matrices were transferred to a new 24-well plate. For the cells to absorb the dye well, the matrices were washed with PBS and stained for one minute with an AO/PI solution prepared at a ratio of 1: 1 (v: v). At the end of the staining protocol, the matrices were washed three times with PBS. Matrix images were examined using an inverted microscope (Olympus IX70 Inverted Microscope, Japan).

As in previous study [20], apoptotic cells were scored in photographs obtained by AO/PI staining, and apoptosis (early and late) inducing potential in cells of different groups was determined as a percentage.

2.8. Cell Viability Analysis

MTT analysis, widely used in the quantitative evaluation of cell viability, was preferred in this study [21]. Briefly, the culture medium was removed from wells at 24, 48, and 72 h. Then, the scaffolds were transferred to the new 24-well plate. For the 10% MTT solution to be used for analysis, 600 µl of DMEM was added to each well in which the matrices were previously placed. Then, 60 µl of MTT solution was carefully injected into the matrices and the plate was left in a gentle shaker for 10 minutes to activate the

solution in the wells. Afterwards, the plate was removed from the incubator for a 4-hour incubation. After incubation, the matrices were taken into a new 24-well plate, and isopropanol alcohol was added to each well. As a result of the interaction, the solutions obtained by carefully crushing and dissolving the formazan crystals in the matrices were taken into clean 96-well wells, and the absorbance was analyzed with a microplate reader (EZ Read 400; Microplate Reader, Biochrom) at wavelength 570 nm. As a control, the MTT method was applied to cell-free scaffolds, and these data were extracted from the values obtained from the cell included matrix.

2.9. Immunostaining

Adhesion molecules play a role in the orientation of cells to tissues, recognizing each other and regulating phenomena such as embryogenesis, cell growth, cell differentiation, and inflammation. By immunocytochemistry staining method, we investigated the presence of pan-cadherin, one of the adhesion molecules, mainly because of its roles in cell-cell and cell-matrix interactions. Briefly, seeded cells into decellularized scaffolds were washed with PBS twice, fixed with methanol for five minutes, and blocked-in blocking serum for 20 minutes. After washing with PBS, cells were incubated with primary antibody (1:100 dilutions, anti-pan cadherin antibody, ab16505, Abcam, UK) overnight. After this duration, cells were washed with PBS and incubated with secondary antibody (1:200 dilutions, goat anti-rat IgG H&L FITC, ab6840, Abcam, UK) for 45 minutes. At the end of this process, DAPI was used for the staining of nuclei, and cell-matrix complexes were examined under an inverted microscope (Olympus IX70 Inverted Microscope, Japan).

2.10. Statistical Analysis

In all experiments, data were represented as a mean ± standard deviation (SD). GraphPad Prism version 5.0 (GraphPad Software Inc., San Diego, CA, USA) was used for statistical analysis. Two-way analyses of variance were conducted to compare results. P values of 0.05 are considered statistically significant. At least three replications of each experiment were conducted.

Results

This study showed that a three-dimensional biomimetic decellularized adipose tissue matrix could be used to model different cancer types in vitro to mimic the cell-cell and cell-matrix interaction of the cancer microenvironment.

2.11. Decellularized Adipose Tissue

Adipose tissue is classified as loose connective tissue and consists of adipocytes. It also has a very thin extracellular matrix layer containing many vessels with

a fiber backbone such as collagen fibers. As a result of the decellularization process applied, a white, dry, and fibrous matrix was obtained from adipose tissue. After H&E staining, no nuclei were found in the matrixes obtained (**Figure 1**). It was also observed by MT staining that the tissue integrity was not impaired (**Figure 1**). Decellularization results showed that the detergent-based method used for the heart in our previous studies yields decellularized ECM scaffolds within the adipose tissue that retain properties similar to their natural structure [12, 13].

2.12. Cell Viability

To compare the viability profile of T98G, Hep3B, and WiDr cancer cells in two- and three-dimensional cultures, an MTT assay was performed on 24th, 48th, and 72nd h (**Figure 2**). The MTT results were examined for differences in cell viability potential between 2D and 3D

and whether there was a difference between different cancer cells in 3D. Cells in two-dimensional cultures exhibited a constant proliferation curve for three days, while each cell type in three-dimensional culture showed a different proliferation profile than in two-dimensional culture. Cancer lines were also found to have different proliferation potentials. In the T98G cell line, a significant increase in viability was observed in 3D compared to 2D at 24 hours (*: $p < 0.05$).

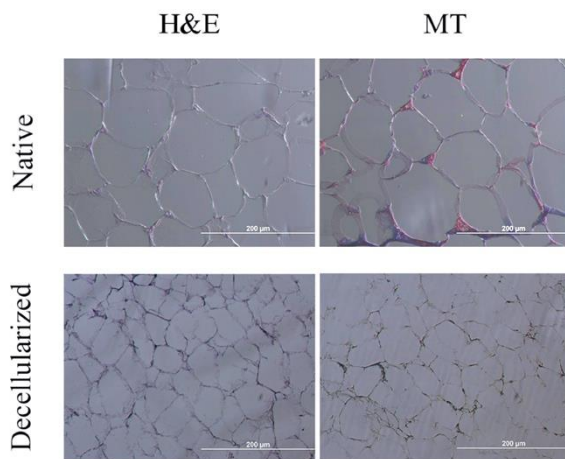


Figure 1. Histological staining of native and decellularized adipose tissue. H&E were used to detect either the presence of residual cells or cell fragments, and MT was used to show collagen content and organization. (H&E: Hematoxylin & Eosin, MT: Masson Trichrome, Scale bar = $\times 10$).

It was observed that the WiDr cell line was much lower in terms of cell viability in the three-dimensional environment than the results obtained in the two-dimensional environment. This difference was found to be significantly lower for all time periods (*: $p < 0.05$).

In Hep3B cell lines, while a decrease was observed in the viability rate in 3D compared to 2D at all hours, it was also determined that this decrease was not statistically significant. Comparing the viability of different cancer cell lines in 3D, it was observed that only T98G cells showed higher cell viability in the matrix at all periods compared to other cell lines (*: $p < 0.05$).

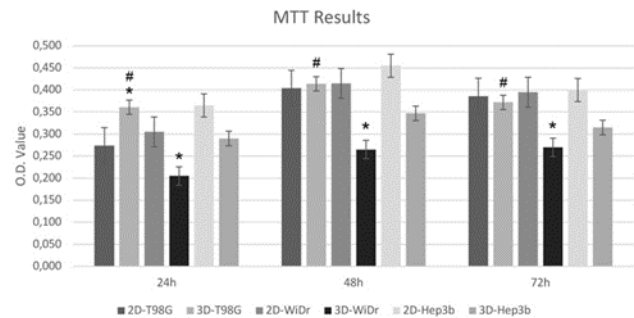


Figure 2. Cell growth potential comparison of the cancer cells in two- and three-dimensional culture. Cell proliferation was measured by MTT assays. Different cancer cells were statistically examined in terms of different time periods within and with each other. (n = 3; h: hours; *: $p < 0.05$, #: $p < 0.05$).

AO/PI staining images were also obtained to support the MTT results (**Figure 3**). Staining in the form of cell aggregates in the matrix was observed, especially in T98G and Hep3B cells at the 24th-hour staining. However, a significant decrease was observed in the number of cells in the matrix at 48th and 72nd h in WiDr cells as seen at Figure 3.

Calculation of the % apoptosis rate was based on the images obtained by AO/PI staining (**Figure 4**). Also, these results support the cell viability potential of results.

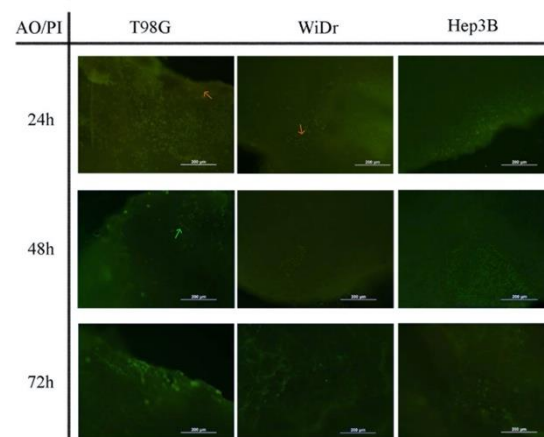


Figure 3. Image of cancer cells on the decellularized adipose matrix at different times. A double staining was performed with AO/PI on the cells. Orange arrows indicate late apoptosis and green arrow live cells. (Magnification: $\times 10$).

2.13. Immunostaining Results

The cell-matrix composition was stained with an anti-pan cadherin antibody to observe cell-cell and cell-ECM interactions after cell lines were seeded into the matrix. Anti-pan cadherin staining results were observed to support the other results obtained. In all cell lines, especially on 24 h images, cellular aggregates bound together were observed within the scaffolds despite poor staining potential (**Figure 5**).

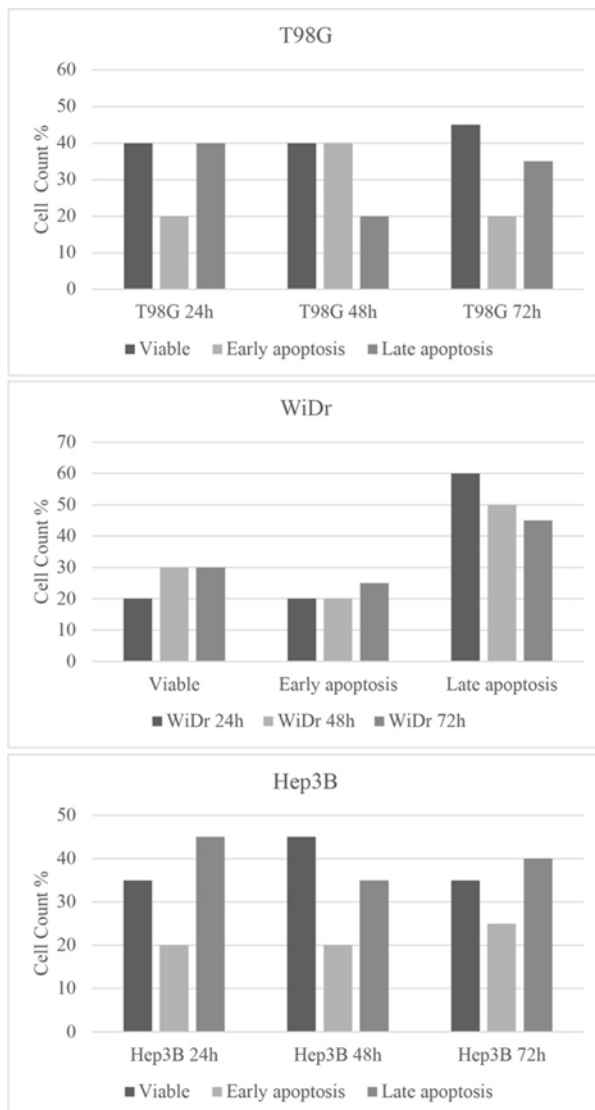


Figure 4. Graph of % apoptosis after AO/PI staining. Calculation of % was made by counting a total of 100 cells from 3 different photographs.

3. Discussion

Successfully designed decellularized tissues and organs should resemble the natural organ in size and structure and have similar biomechanical properties to these structures. It should also not induce an immunogenic response and should be able to support cell proliferation [22, 23].

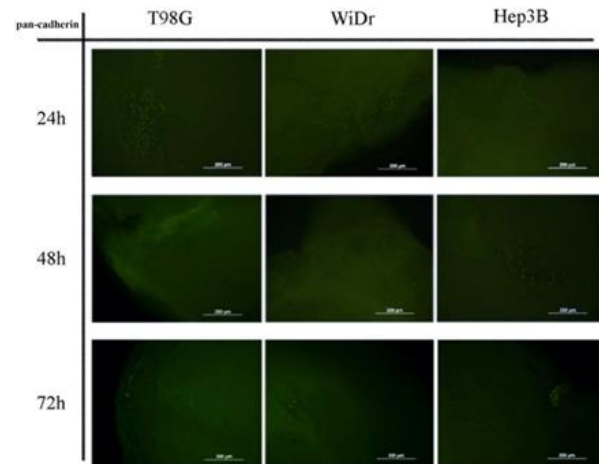


Figure 5. Pan-cadherin immunostaining of adipose matrix at different times (Magnification: $\times 10$).

In different studies, models known as chimeric, human cells on matrices obtained from different species have been tested, as well as studies in which matrix-cell interactions obtained from the same species are examined [18, 24]. The reason for this is the absence of immune cells in the matrices obtained by the decellularization process. Accordingly, detergent-based decellularization was used to decellularize rat adipose tissue within the scope of this study. Proliferation profiles of different cancer cell lines (T98G, WiDr, and Hep3B) were investigated on these matrices.

The ECM scaffolds that are naturally derived are ideal candidates for tissue engineering applications. This is in large part because the ECM establishes cell-cell and cell-matrix relationships while organizing cellular functions like differentiation and proliferation [18, 24]. Since adipose tissue is abundant in the body, it is widely used in tissue engineering as a source of ECM [25]. An extracellular matrix derived from human adipose tissue (hDAM) was employed in a previous study to study breast cancer growth, with the results showing that this system functions like a biomimetic microenvironment for cancer cells [18]. Dunne et al. [18] and Chaitin et al. [24] used both physical and chemical decellularization methods in their studies, whereas only chemical decellularization method was used in the current study. The most important difference between these two methods is that the damage that can be caused by the physical decellularization method in the extracellular matrix is minimized [18, 24]. At the same time, the short duration of the method used in the present study is an important factor for maintaining the integrity of the ECM. In our study, different from the studies mentioned above, different cancer cell types were examined. As a result of the literature review, no study was found with these cell types in terms of their adhesion capacity and cellular behavior on the decellularized adipose tissue matrix.

Various methods have been proposed and compared in the literature for the decellularization of adipose tissue [26, 27]. In this study, the detergent method we standardized in our previous studies was applied [12-14]. The most important difference of this method from other decellularization methods is its reduced application time and efficiency. These features of the detergent method made us think it might be preferable in the adipose tissue engineering approach, mainly because of the sensitive ECM of adipose tissue. In this study, decellularization results showed that dry, white, fibrous, and porous scaffolds were obtained. It was observed that the tissue structure was preserved, and the proliferative potential of different cancer cell lines had a profile close to the two-dimensional culture medium. AO/PI staining results also supported cell viability analysis.

Decellularized matrices of organs can serve as promising platforms for building in vitro cancer models. Its advantages include the specificity of the molecular composition of a particular organ and the preservation of tissue integrity; these properties allow for simulating the tumorigenesis processes with a high degree of affinity [28].

We used T98G, WiDr, and Hep3B cell lines to evaluate the ability to sustain cancer cell proliferation in the decellularized adipose matrixes we obtained. We have observed that the recellularization process is reproducible and reliable, but different cancer cells colonize the scaffold differently (**Figures 3 and 4**). In the three-dimensional matrix model, we observed that the tumor cells are located on the edge surfaces of the matrix. Moreover, in immunocytochemistry analyzes, we observed that cell-cell and cell-matrix interactions differ according to the proliferation potential of tumor cells in ECM. It was observed that T98G and Hep3B cells were more common in the margins of the matrix surface due to their easier access to nutrients and oxygen. This behavior of cells can be explained by the relationship between the location of the tumor tissue in the body close to the capillaries and the active proliferation power of cancer cells thanks to this location. The proliferation potential of T98G and Hep3B cells continued on the third day. This result showed that the decellularized scaffold has a cytocompatibility structure. The tissue architecture well preserved on AO/PI staining suggested that these cells have a much higher capacity for cell adhesion potential. However, the possibility of cells being deep in the tissue and not imaging with fluorescent staining is the limiting part of the study. Further studies (such as electron microscopic examination) are required to demonstrate cells embedded in the ECM.

4. Conclusion

As a result, it is seen that the porous structure of the adipose tissue matrix obtained by the chemical decellularization method preserves its natural ECM properties, and this tissue matrix can mimic the desired cancer tissue microenvironment. Removing cellular contents from the tissue with the shortest processing time showed the method's effectiveness. The reduced processing time and the applicability of the method can make it a preferable method in decellularization methods. It was thought that the proliferation profile of T98G, WiDr, and Hep3B in these scaffolds should be examined for longer periods, and these scaffolds should be obtained from different tissues and tested according to the cancer model. Likewise, it can be said that studies should be designed considering that different cancer cells showed different proliferation behaviors on decellularized matrices and that the compatibility of cancer cells and matrix may differ in the in vitro model to be designed for this.

Acknowledgement

The author did not receive any specific grant for this research from any funding agency in the public, commercial, or not-for-profit sectors.

Author's Contributions

Esin Akbay Çetin: Conceptualized the study, performed the experiments and analyses of result, drafted and wrote the manuscript.

Ethics

In this study animal was used for experiment with the approval of the Hacettepe University Animal Care and Use Committee (Permit no. 2012/52).

References

- [1]. Kocarnik, J. M., Compton, K., et al., 2022, Cancer incidence, mortality, years of life lost, years lived with disability, and disability-adjusted life years for 29 cancer groups from 2010 to 2019: a systematic analysis for the global burden of disease study 2019. *JAMA Oncology*, 8: 420-444.
- [2]. Han, S. J., Kwon, S., Kim, K. S., 2022, Contribution of mechanical homeostasis to epithelial-mesenchymal transition. *Cellular Oncology*, 45:1119-1136.
- [3]. Walker, C., Mojares, E., del Río Hernández, A., 2018, Role of extracellular matrix in development and cancer progression. *International Journal of Molecular Sciences*, 19:3028.
- [4]. Sensi, F., D'Angelo, E., et al., 2020, Recellularized colorectal cancer patient-derived scaffolds as in vitro pre-clinical 3D model for drug screening. *Cancers*, 12:681.

- [5]. Brancato, V., Oliveira, J.M., et al., 2020, Could 3D models of cancer enhance drug screening?. *Biomaterials*, 232:119744.
- [6]. Pospelov, A.D., Timofeeva, L.B., et al., 2020, Comparative analysis of two protocols of mouse tissues decellularization for application in experimental oncology. *Opera Medica et Physiologica*, 7:13.
- [7]. Ferreira, L.P., Gaspar, V.M., 2020, Decellularized extracellular matrix for bioengineering physiometric 3D in vitro tumor models. *Trends in Biotechnology*, 38:1397-1414.
- [8]. Rijal, G., Li, W., 2018, Native-mimicking in vitro microenvironment: an elusive and seductive future for tumor modeling and tissue engineering. *Journal of Biological Engineering*, 12:1-22
- [9]. Mavrogatou, E., Pratsinis, H., et al., 2019, Extracellular matrix alterations in senescent cells and their significance in tissue homeostasis. *Matrix Biology*, 75:27-42.
- [10]. Theocharis, A.D., Karamanos, N.K., 2019, Proteoglycans remodeling in cancer: Underlying molecular mechanisms. *Matrix Biology*, 75:220-259.
- [11]. Ajeti, V., Lara-Santiago, J., et al., 2017, Ovarian and breast cancer migration dynamics on laminin and fibronectin bi-directional gradient fibers fabricated via multiphoton excited photochemistry. *Cellular and Molecular Bioengineering*, 10:295-311.
- [12]. Sesli, M., Akbay, E., Onur, M. A., 2018, Decellularization of rat adipose tissue, diaphragm, and heart: a comparison of two decellularization methods. *Turkish Journal of Biology*, 42:537.
- [13]. Akbay, E., Onur, M. A., 2019, Investigation of survival and migration potential of differentiated cardiomyocytes transplanted with decellularized heart scaffold. *Journal of Biomedical Materials Research Part A*, 107:561-570.
- [14]. Akbay, E., Onur, M. A., 2018, Myocardial Tissue Engineering: A Comparative Study of Different Solutions for Use as a Natural Scaffold Being of Heart a Comparative Study of Different Solutions for Decellularization Heart Scaffold. *Biomedical Journal*, 2:4.
- [15]. Thevenot, P., Nair, A., et al., 2008, Method to analyze three-dimensional cell distribution and infiltration in degradable scaffolds. *Tissue Engineering Part C Methods*, 14:319-31.
- [16]. Lim, P.J., Gan, C.S., et al., 2019, Lipid lowering effect of *Eurycoma longifolia* Jack aqueous root extract in hepatocytes. *Kuwait Journal of Science*, 46: 2.
- [17]. Wang, L., Johnson, J.A., et al., 2013, Combining decellularized human adipose tissue extracellular matrix and adipose-derived stem cells for adipose tissue engineering. *Acta Biomaterialia*, 9:8921-31.
- [18]. Dunne, L.W., Huang, Z., et al., 2014, Human decellularized adipose tissue scaffold as a model for breast cancer cell growth and drug treatments. *Biomaterials*, 35:4940-49.
- [19]. Tığlı, S.R., Ghosh, S., et al., 2009, Comparative chondrogenesis of human cell sources in 3D scaffolds. *Journal of Tissue Engineering and Regenerative Medicine*, 3:348-60.
- [20]. Abdel Wahab, S.I., Abdul, A.B., et al., 2009, In vitro ultramorphological assessment of apoptosis induced by Zerumbone on (HeLa). *Journal of Biomedicine and Biotechnology*, 2009.
- [21]. Mosmann, T., 1983, Rapid colorimetric assay for cellular growth and survival: application to proliferation and cytotoxicity assays. *Journal of Immunological Methods*, 65:55-63.
- [22]. Gubareva, E.A., Sjöqvist, S., et al., 2016, Orthotopic transplantation of a tissue engineered diaphragm in rats. *Biomaterials*, 77:320-35.
- [23]. Fisher, M.F., Rao, S.S., 2020, Three-dimensional culture models to study drug resistance in breast cancer. *Biotechnology and Bioengineering*, 117:2262-78.
- [24]. Chaitin, H., Lu, M.L., et al., 2021, Development of a decellularized porcine esophageal matrix for potential applications in cancer modeling. *Cells*, 10:1055.
- [25]. Flynn, L.E., 2010, The use of decellularized adipose tissue to provide an inductive microenvironment for the adipogenic differentiation of human adipose-derived stem cells. *Biomaterials*, 31:4715-24.
- [26]. Brown, B.N., Freund, J.M., et al., 2011, Comparison of three methods for the derivation of a biologic scaffold composed of adipose tissue extracellular matrix. *Tissue Engineering Part C Methods*, 17:411-21.
- [27]. Chun, S.Y., Lim, J.O., et al., 2019, Preparation and characterization of human adipose tissue-derived extracellular matrix, growth factors, and stem cells: a concise review. *Tissue Engineering and Regenerative Medicine*, 16:385-93.
- [28]. Varol, C., Sagi, I., 2018, Phagocyte-extracellular matrix crosstalk empowers tumor development and dissemination. *The FEBS Journal*, 285:734-51.